Four Wave Mixing Oscillation in a Semiconductor Microcavity: Generation of Two Correlated Polariton Populations

M. Romanelli, C. Leyder, J. Ph. Karr, E. Giacobino, and A. Bramati

Laboratoire Kastler Brossel, Université Paris 6, Ecole Normale Supérieure et CNRS, UPMC Case 74, 4 place Jussieu, 75252 Paris Cedex 05, France

(Received 15 December 2005; published 7 March 2007)

We demonstrate a novel kind of polariton four wave mixing oscillation. Two pump polaritons scatter towards final states that emit two beams of equal intensity, separated both spatially and in polarization with respect to the pumps. The measurement of the intensity fluctuations of the emitted light demonstrates that the final states are strongly correlated.

DOI: 10.1103/PhysRevLett.98.106401 PACS numbers: 71.36.+c, 42.50.−p, 42.70.Nq, 71.35.Gg

In strong-coupling semiconductor microcavities [1] the system is described in terms of ''mixed'' exciton-photon quasiparticles, the cavity polaritons. These composite bosons have very interesting properties [2]. The exciton part is responsible for the coupling between polariton modes via the Coulomb interaction, which is at the origin of polaritonic nonlinearities. The understanding of these nonlinearities was greatly improved by the results of Refs. [3,4]. In the presence of a pump beam resonant with polaritons having a wave vector $\mathbf{k_p}$, Ref. [3] demonstrated parametric amplification of a probe beam at normal incidence and emission of a weak ''idler'' beam with wave vector $2\mathbf{k_p}$. Reference [4] evidenced the coherence properties of the emission, which confirmed the parametric nature of the process. The nonlinear mechanism is thus parametric scattering of two polaritons from the pump mode into a signal-idler pair $\{\mathbf{k_p}, \mathbf{k_p}\} \Rightarrow \{\mathbf{0}, 2\mathbf{k_p}\}$ [5]. The system has many similarities with an optical parametric oscillator (OPO) [6], further emphasized by the demonstration of parametric oscillation [7] and optical bistability [8]. A remarkable property of OPOs above the oscillation threshold is the generation of two bright quantum correlated beams [9]. In principle, polariton parametric oscillation should lead to the same effect and generate two macroscopically populated polariton modes (the signal and idler polaritons) which are quantum correlated [10,11]. However, a major problem arises because of the asymmetry between the signal and idler modes. Because of its large wave vector, the idler polariton has a small photonic fraction and the idler beam has a much weaker intensity than the signal beam (the intensity ratio is typically $\sim 10^{-2}$–10^{-4} [7,12,13]). This makes it very difficult to measure the correlations of the signal and idler. Even though a signature of quantum pair correlations has been recently shown in the regime of multimode parametric scattering below the oscillation threshold [14], to the best of our knowledge a direct evidence of signal-idler correlations in the oscillation regime is lacking. Balanced signal and idler beams have been generated recently with a single pump in a system involving a triple microcavity, but no correlation measurements have been performed [15].

In this Letter, we describe a polariton four wave mixing oscillator that generates balanced signal and idler beams. We use the parametric scattering of two pumps with opposite wave vectors to generate two symmetric signal and idler polaritons $\{\mathbf{k_p}, -\mathbf{k_p}\} \Rightarrow \{\mathbf{k}, -\mathbf{k}\}$. Above the oscillation threshold the two beams have the same intensities since they are produced by polariton states having opposite wave vectors, and hence they have the same photonic fraction and linewidth. The emitted beams are spatially separated and linearly polarized. Furthermore, their polarization is orthogonal with respect to the pump polarization, in agreement with other recent observations [16–18]. The direction of the emission is linked to the crystal lattice orientation. These features simplify the optical detection, since they permit to filter out the pump light and part of the secondary emission produced by elastic scattering (resonant Rayleigh scattering). We have measured the intensity correlations of the two beams, finding that almost perfect correlations are present. In the strong-coupling regime, extracavity photon fields carry the amplitude and phase information of the intracavity polariton fields; therefore, our results demonstrate the generation of two strongly correlated macroscopic polariton populations, in which the electronic excitations in the semiconductor quantum well are involved.

The experimental setup is shown in Fig. 1(a). We use two pump beams resonant with the lower polariton branch, having opposite in-plane wave vectors $\{\mathbf{k_p}, -\mathbf{k_p}\}$. For cross scattering processes involving one polariton from each pump mode, momentum conservation requires that the signal and idler have opposite wave vectors, while energy conservation imposes $|\mathbf{k}| = |\mathbf{k_p}|$. As a consequence, all pair scattering processes $\{\mathbf{k_p}, -\mathbf{k_p}\} \Rightarrow \{\mathbf{k}, -\mathbf{k}\}$ with the condition $|\mathbf{k}| = |\mathbf{k_p}|$ are, in principle, allowed.

Nonlinear emission is expected on a circle in the far-field plane, whose diameter is fixed by the pump wave vector [see Fig. 1(b)]. The incidence angle of the pump beams is about 6°. This value is chosen so as to avoid competition with the one-pump scattering channel $\{\mathbf{k_p}, \mathbf{k_p}\} \Rightarrow \{\mathbf{0}, 2\mathbf{k_p}\}$, the efficiency of which is maximal

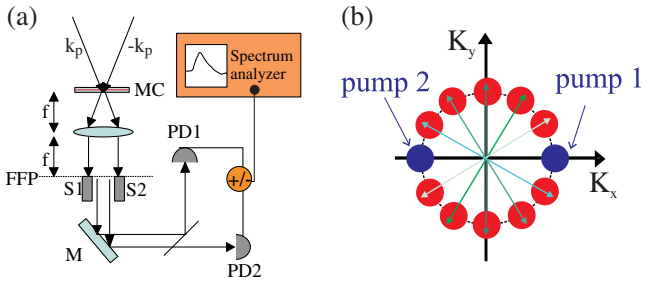

FIG. 1 (color online). (a) Experimental setup. Two pump beams $\mathbf{k_p}$ and $-\mathbf{k_p}$ are focused on the microcavity sample MC. The microcavity emission is collimated by a lens ($f = 50$ mm). Two movable screens $S1$ and $S2$ placed in the far field plane (FFP) eliminate the transmitted pump beams. The upper part of the emission is detected by photodiode PD1, the lower part by photodiode PD2. The photocurrent sum and difference are then spectrally analyzed. (b) Representation in k space of the expected scattering processes. Correlated pairs are connected by arrows.

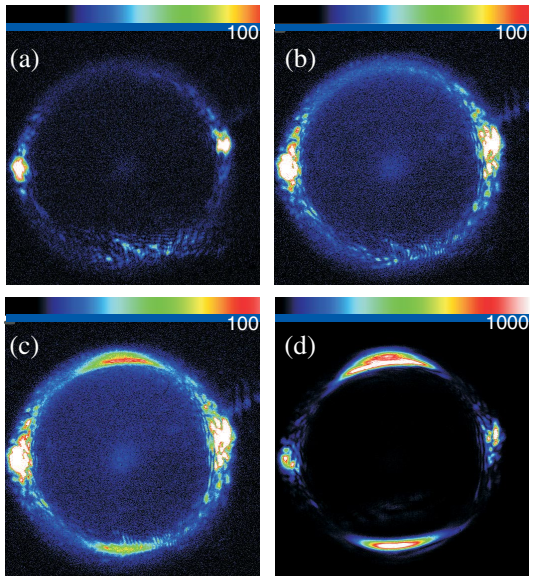

FIG. 2 (color online). (a) Far-field emission in the TE polarization for a total pump power of: (a) 3 mW, (b) 19 mW, (c) 27 mW, (d) 39 mW. Cavity-exciton detuning $\delta = 0$. At low pump power (a)–(b), light intensity is roughly uniform on the elastic circle (except for the two pump spots, lying approximately on the horizontal diameter). At high pump power (c)–(d), scattered polaritons accumulate around the $\mathbf{k_y}$ diameter.

at the so-called "magic angle", i.e., about 12° for this sample. The two linearly TM-polarized (polarization in the incidence plane) pumps are focused on the microcavity sample on a spot of 80 μm in diameter. The polarization-resolved far-field emission is studied in transmission using a 50 mm lens and a CCD camera. Two independently movable screens allow to select a part of the far-field emission, which is subsequently detected by two identical photodiodes. The two photocurrents are amplified and their sum or difference is sent to a spectrum analyzer. The microcavity sample is cooled at 4 K in a cold finger cryostat. The sample is described in detail in Ref. [19]. It is a high quality factor 2λ GaAs/AlAs cavity, with three low indium content $In_{0.04}Ga_{0.96}As$ quantum wells, one at each antinode of the cavity mode. The Rabi splitting energy is 5.1 meV. Polariton linewidths are in the 100–200 μeV range. The laser source is a cw Ti:Sa laser, intensity stabilized, with 1 MHz linewidth.

In Fig. 2 we show the far-field emission detected on the TE-linear polarization, orthogonal to the pump polarization, for several values of the pump power. For low pump power (a)–(b), the emitted TE-polarized light is weak and roughly uniformly distributed on the elastic circle. For higher pump power (c–d), two bright spots located on the $\mathbf{k_y}$ diameter appear, breaking the circular symmetry of the emission. This novel feature is a strong indication that the oscillation threshold has been reached. Above threshold, polaritons do not redistribute uniformly over the elastic circle; rather, they scatter preferentially towards states localized around a well-defined diameter, the $\mathbf{k_y}$ one. As a result, two macroscopic polariton populations build up in these states [Fig. 2(c) and 2(d)]. This emission exhibits the primary features of parametric oscillation, since the energy and momentum of the pumps are conserved. In addition, if the light is detected with a polarization parallel to that of the pumps, no bright spots and no threshold are observed, showing polarization inversion linked to polariton-polariton scattering, in agreement with previous studies [16–18].

The fact that the $\mathbf{k_y}$ diameter is the privileged one for stimulated scattering is also evidenced. In order to better understand the origin of this feature, we rotated the sample, keeping the same experimental conditions: we observed that the selected diameter rotates accordingly. This effect can then be related to the fact that the $\mathbf{k_y}$ diameter coincides with the [110] crystal axis, which introduces a preferred direction. No emission threshold was observed along the other crystal axis. Further investigations of the symmetry properties of the emission process, in connection with theoretical modeling, will be necessary to fully account for this effect.

In Fig. 3, we show the optical power emitted by the upper and lower polariton populations, integrated over the emission zone [see Fig. 3(a)], as a function of the pump power. Oscillation threshold is reached at a pump power of about 20 mW. By "pump power," we mean the sum of the powers of the pump beams. Right above threshold the emission increases very rapidly with the pump power. Then the slope decreases and is expected to go towards 0, 5 well above threshold, as in a standard OPO. However, thermal effects in the sample prevent from checking this point precisely. Above threshold, the powers of the two emitted beams are almost equal (within 10%). We stress that this situation is very different from the conventional

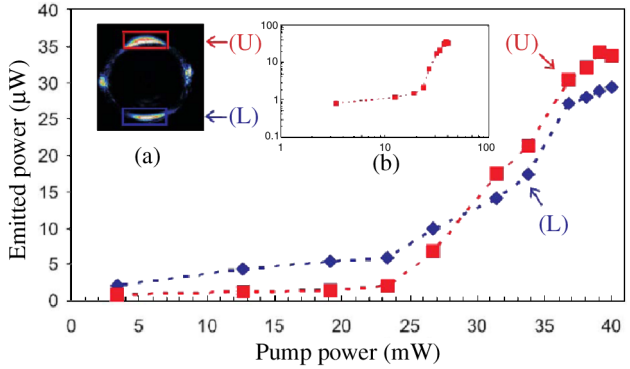

FIG. 3 (color online). Optical power of the upper (U) and lower (L) beam as a function of the pump power. Cavity-exciton detuning $\delta = 0$. Inset (a) the zones over which the upper and lower emissions are, respectively, integrated are shown. Inset (b) log-log plot of the upper beam emission as a function of pump power.

"magic-angle" configuration, where the signal beam is 10^2–10^4 times stronger than the idler [7,12,13]. Below threshold there is a significant imbalance due to the fact that only a small fraction of the emission in this range is due to four wave mixing, as evidenced by the correlation measurements (see below).

In the case of four wave mixing emission, the two conjugate beams are expected to exhibit extremely strong intensity correlations, since every scattering process from the two pumps create two polaritons, one in each of the states on the $\mathbf{k}_y$ diameter, in order to fulfill energy and momentum conservation. We have verified this feature by measuring the intensity correlations of the two beams. In order to do so, we have detected the beams with two identical photodiodes. The generated photocurrents are electronically added or subtracted; the noise spectra of the photocurrent sum and difference are measured with a spectrum analyzer, as shown in Fig. 1.

In all the experiments described here, the analysis frequency is fixed at the same value of 4 MHz. We did not observe any frequency dependence in the experimentally available frequency range (2–30 MHz). This is due to the fact that the width of the correlation spectrum is expected to be of the same order as the width of the polariton resonance, i.e., a few tens of GHz. The normalized intensity correlation between the beams $\{\mathbf{k}, -\mathbf{k}\}$ is defined as

$$C_{\mathbf{k},-\mathbf{k}}(\Omega) = \frac{S_{\mathbf{k},-\mathbf{k}}(\Omega)}{\sqrt{S_{\mathbf{k}}(\Omega) S_{-\mathbf{k}}(\Omega)}}, \qquad (1)$$

where $S_{\mathbf{k},-\mathbf{k}}$ is the intensity correlation spectrum (defined as the Fourier transform of the correlation function $C_{\mathbf{k},-\mathbf{k}}(\tau) = \langle \delta I_{\mathbf{k}}(t) \delta I_{-\mathbf{k}}(t+\tau) \rangle$) and $S_{\mathbf{k}}$, $S_{-\mathbf{k}}$ are the intensity noise spectra of the two beams (defined as the Fourier transform of the intensity autocorrelation function $C_I(\tau) = \langle \delta I(t) \delta I(t+\tau) \rangle$). This quantity always verifies $|C_{\mathbf{k},-\mathbf{k}}(\Omega)| \leq 1$ and is equal to 1 for perfect correlations and -1 for perfect anticorrelations.

One can have access to the normalized intensity correlation $C_{\mathbf{k},-\mathbf{k}}$ by measuring the noise spectra of the intensity sum S_+, of the intensity difference S_-, and of each beam $S_{\pm\mathbf{k}}$. These quantities satisfy the following equation:

$$C_{\mathbf{k},-\mathbf{k}} = (S_+ - S_-)/4\sqrt{S_{\mathbf{k}} S_{-\mathbf{k}}}. \qquad (2)$$

The normalized intensity correlation is plotted as a function of pump power in Fig. 4(b). One recognizes a clear threshold behavior in the correlation coefficient: for low pump powers the correlation is weak, while it jumps abruptly to values close to 1 for a pump power of about 15 mW. Above this value, the correlation does not exhibit a

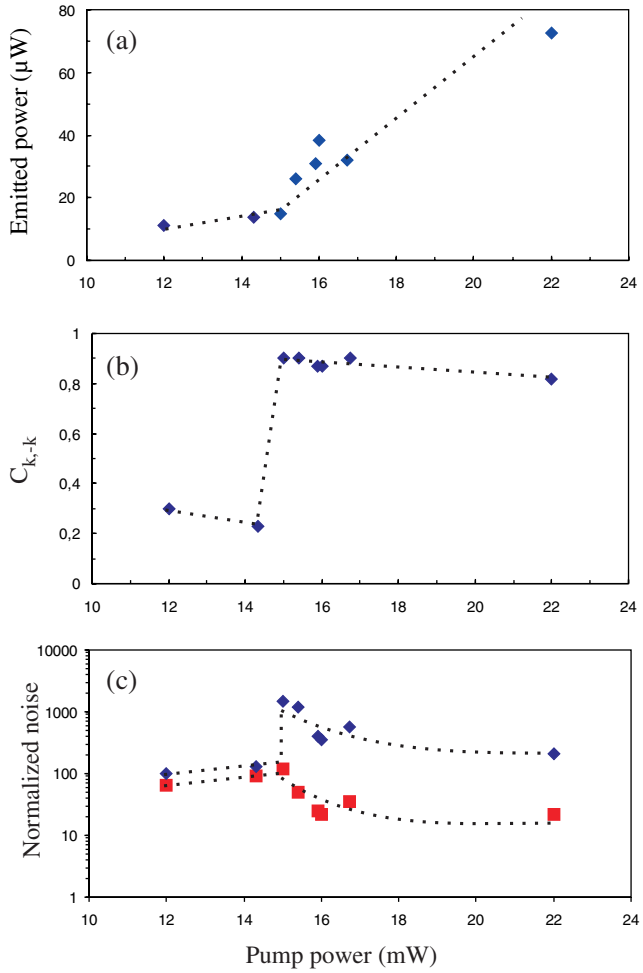

FIG. 4 (color online). (a) Four wave mixing optical power as a function of the pump power. The threshold value of the pump power and the average emitted power differ from those reported in Fig. 3, because the two sets of data were taken in slightly different experimental conditions. (b) Normalized intensity correlation $C_{\mathbf{k},-\mathbf{k}}$ as a function of the pump power. (c) Noise of photocurrent sum S_+ and of photocurrent difference S_- (normalized to the standard quantum limit) as a function of the pump power. In all curves, dashed lines are guides to the eye.

marked dependence on the pump power. By comparing Fig. 4(b) with the emitted average power for this series of experimental data [Fig. 4(a)], one can see that the correlation increases abruptly at the four wave mixing oscillation threshold.

Such a high value of $C_{\mathbf{k},-\mathbf{k}}$ proves that polariton four wave mixing allows the generation of two macroscopic polariton populations that are strongly correlated. Note that the correlations cannot in any way be due to the fact that the two pump beams are produced by the same laser. We have carefully checked that the intensity fluctuations of the two pump beams are completely uncorrelated at the frequency of analysis of 4 MHz. This is due to the fact that the noise level of the pump laser is the standard quantum limit (at the frequencies of the noise measured in the experiment). Therefore, the pump beams cannot be at the origin of the correlations between the two emitted beams. Correlations are instead generated by the four wave mixing process.

As is apparent from Eq. (2), the correlation coefficient is connected to the noise of the sum and difference, S_+ and S_-, of the detected photocurrents. Below oscillation threshold, the noises of sum and difference are quite the same, indicating poor correlations. At threshold, the sum noise increases abruptly, while the difference noise decreases, showing evidence for the emergence of strong correlations. As the pump power is further increased, the emission noise decreases, as expected in any oscillator far from threshold. The noise on the sum as well as on the difference decreases and the correlations remain high.

While above threshold, high correlations are observed, as expected for a parametric oscillator, the behavior below threshold differs from what is expected for a standard OPO;, in particular, OPOs exhibit strong correlations below threshold, which is not the case in our system. This indicates that the few μW of optical power detected below threshold [see Fig. 3 and 4(a)] comprise only a very weak contribution from parametric luminescence (otherwise they would be strongly correlated); the major contribution comes instead from other processes, such as Rayleigh scattering and resonant incoherent luminescence [20]. This gives an uncorrelated background, which is dominant at low pump power. Above threshold, as the four wave mixing process becomes efficient and generates correlated polaritons, the noise level on the difference is strongly reduced. However, the presence of the uncorrelated background is responsible for the residual noise on the intensity difference and prevents the system from approaching the quantum regime.

Therefore, present results are expected to be improved in a configuration in which the FWM emission is not exactly at the same energy as the pumps [14], and do not lie on the elastic circle, where the background emission is expected to be the strongest.

In conclusion, we have demonstrated a novel kind of polariton parametric four wave mixing oscillation. In contrast with the so-called magic-angle configuration, our scheme is based on the parametric interaction of two distinct pump modes with opposite wave vectors. We have shown that above the oscillation threshold, pump polaritons scatter towards final states orthogonally polarized with respect to the pumps, and localized around a well-defined diameter of the elastic circle in the far field. Furthermore, we have demonstrated for the first time that the final states of the scattering process are strongly correlated. Our results indicate that the achievement of quantum correlated and entangled polaritons may be within reach in the near future.

We acknowledge enlightening discussions with A. Kavokin, G. Malpuech, and C. Ciuti. We are very grateful to R. Houdré for providing us with the microcavity sample, and to G. Leuchs for ultralow noise photodetectors.

[1] C. Weisbuch *et al.*, Phys. Rev. Lett. **69**, 3314 (1992).
[2] A. Kavokin and G. Malpuech, *Cavity Polaritons* (Elsevier, New York, 2003); Special Issue on Microcavities, edited by J. J. Baumberg and L. Viña [Semicond. Sci. Technol. **18**, S279 (2003)]; Special Issue on Physics of Semiconductor Microcavities, edited by B. Deveaud [Phys. Status Solidi B **242**, 11 (2005)].
[3] P. G. Savvidis *et al.*, Phys. Rev. Lett. **84**, 1547 (2000).
[4] G. Messin *et al.*, Phys. Rev. Lett. **87**, 127403 (2001).
[5] C. Ciuti *et al.*, Phys. Rev. B **62**, R4825 (2000).
[6] J. J. Baumberg *et al.*, Phys. Rev. B **62**, R16247 (2000).
[7] R. M. Stevenson *et al.*, Phys. Rev. Lett. **85**, 3680 (2000).
[8] A. Baas *et al.*, Phys. Rev. B **70**, 161307(R) (2004).
[9] A. Heidmann *et al.*, Phys. Rev. Lett. **59**, 2555 (1987).
[10] J.-Ph. Karr, A. Baas, and E. Giacobino, Phys. Rev. A **69**, 063807 (2004).
[11] P. Schwendimann, C. Ciuti, and A. Quattropani, Phys. Rev. B **68**, 165324 (2003).
[12] M. Saba *et al.*, Nature (London) **414**, 731 (2001).
[13] R. Butté *et al.*, Phys. Rev. B **68**, 115325 (2003).
[14] S. Savasta *et al.*, Phys. Rev. Lett. **94**, 246401 (2005).
[15] C. Diederichs *et al.*, Nature (London) **440**, 904 (2006).
[16] K. V. Kavokin *et al.*, Phys. Status Solidi C **2**, 763 (2005).
[17] P. Renucci *et al.*, Phys. Rev. B **72**, 075317 (2005).
[18] G. Dasbach *et al.*, Phys. Rev. B **71**, 161308(R) (2005).
[19] R. Houdré *et al.*, Phys. Rev. Lett. **85**, 2793 (2000).
[20] R. P. Stanley *et al.*, Phys. Rev. B **55**, R4867 (1997); G. R. Hayes *et al.*, Phys. Rev. B **58**, R10175 (1998).